

## DEVELOPMENT AND VALIDATION OF COMPUTER MODELS FOR STRUCTURES IN JOINTED ROCK

PAUL E. SENSENY<sup>1\*</sup> AND THOMAS A. PUČIK<sup>2</sup>

<sup>1</sup>*Factory Mutual Research Corporation, Norwood, MA 02062, U.S.A.*

<sup>2</sup>*Logicon RDA, Los Angeles, CA 90045, U.S.A.*

### SUMMARY

An extensive program was conducted to develop and validate computer models for the deformation of structures in jointed rock. Both discrete element and finite element models were investigated. The program comprised a sequence of seven calculational and experimental studies. In the final step, model predictions were compared with experimental data from a well-instrumented jointed-rock precision test. The results show that the sophisticated models developed were able to predict some elements of structural deformation in jointed rock, but that it is difficult to make high-confidence predictions of all aspects of structural deformation with these models. Copyright © 1999 John Wiley & Sons, Ltd.

Key words: finite element model; dynamic; jointed rock; tunnel; verification; validation

### INTRODUCTION

Computer models are increasingly being used to analyse the response of structures in jointed rock to various loads.<sup>1–11</sup> These models provide the capability to analyse situations involving layouts, geologies and stress conditions that are not amenable to empirical<sup>12–14</sup> or observational<sup>15</sup> methods. Analytical design methods calculate the stress and deformation for an opening based on details of the geology and reinforcement, basic conservation laws as well as mechanistic models for rock deformation and failure. To date, these methods have been the least used in engineering practice because of the difficulty in prescribing the input data and because of the low confidence in the mechanistic models for deformation and strength of jointed rock. With the increased power of computers and the use of advanced site characterization methods, the prospect of reduced risk and improved cost control using analytical design methods is rapidly expanding.

The growing use of these models is generating a need for greater reliability in the answers they produce. Large, sophisticated computer models can give a false sense of confidence because of the implied level of accuracy in the simulations. The individual components of the methodology: site characterization, mechanics of intact rock behaviour and mechanics of joint behaviour need to be validated. Also, the overall computer models, including domain size, boundary conditions and initial conditions, need to be validated so that predictions of analytical models can be confidently used to design an opening.

\*Correspondence to: P. E. Senseny, Factory Mutual Research Corporation, Norwood, MA 02062-9102, U.S.A.

†Formerly, Defense Special Weapons Agency, Alexandria, VA 22310, U.S.A.

Validation, especially of the overall models, is difficult because of the scarcity of data that have the accuracy and precision needed to be confident that the analytical model gives the correct answer. In general, rock mechanics problems are perceived as data limited because the data needed are often unavailable or not easily obtained.<sup>16</sup> To address this shortfall, a very precise experiment was performed to investigate the influence of joints on the deformation of an opening when the geometry and properties of the joints are exactly known.<sup>17,18</sup> The test was conducted on a large-scale model of jointed-rock geology that contained a lined circular tunnel. The test results are self-consistent and permit the data to be used to validate computational models for the mechanics of structural deformation and failure in jointed rock.

This paper describes the sequence of steps taken to develop computer models for structural deformation in jointed rock and to validate the models using data from the jointed-rock precision test described above. The comparisons with test data and observed modelling sensitivities show that sophisticated models can predict some features of structural deformation in jointed rock, but that it is difficult to make high-confidence predictions with these models without further development. The paper also gives observations on some important aspects of the development and validation process.

### PRELIMINARY REMARKS

The primary objective of this work was to develop and to validate computer models for structures in jointed rock. To place this in context, it is important to distinguish between mathematical models and computer codes, as well as between verification and validation.

A *mathematical model* is a set of mathematical equations intended to describe physical reality. In mechanics, the mathematical model includes the conservation equations for mass, momentum, and (sometimes) energy, the specification of the spatial domain, the initial conditions within the domain, the boundary conditions on the domain, and equations describing the constitutive behaviour of the material(s) within the domain. A *computer code* is an automated procedure for solving the equations prescribed in the mathematical model, usually by numerical means. The codes used for mechanics problems typically include methods for discretizing the equations in space and time, along with algorithms for solving the approximate equations that result.

*Verification* is the process of testing a computer code to insure that the answers it gives are consistent with the mathematical model that was prescribed. In principle, this is a purely mathematical problem that can be addressed by purely mathematical means, such as comparing the predictions of a given code to known closed-form solutions, to 'numerically exact' solutions, to the predictions of other codes, and by mesh refinement studies. *Validation* is the process of testing the mathematical model (typically in combination with a verified computer code) to insure that the answers it gives are consistent with the physical reality it is intended to represent. In practice, this can only be done by comparing model predictions to experimental data of sufficiently high quality and precision to allow sensible conclusions to be drawn and choices to be made between different modelling alternatives.

Despite the best verification and validation efforts, it is sometimes found that different models give appreciably different results for supposedly identical problems. In many cases this can be traced to inappropriate inputs by inexperienced users. For example, the mesh refinement used in an analysis is controlled by the user, not by the code itself. A common problem with inexperienced users is that they use too coarse a mesh to save execution time, or they fail to recognize the need for additional refinement in areas with high gradients. In other cases, it can be traced to

differences in the underlying mathematical models, especially the constitutive models. Under the right conditions, even seemingly small differences in the models can lead to large differences in the predicted results. In some rare cases, the differences have been traced to previously undiscovered bugs in a code.

Most of the code results presented in this paper were generated using well-tested, verified codes run by experienced users who were very familiar with their respective codes. However, there were some differences in the models that were employed, especially the constitutive models and the joint models. In some cases, these differences led to appreciable differences in predicted results, with some predictions being significantly better (or worse) than others.

In the following discussion, the names of the computer codes are used to identify both the codes and the particular mathematical models. Except for a few cases that are clearly identified, failures or shortfalls in the results represent failures of the mathematical models, and not of the computer codes themselves. Therefore, except where noted, the current results are neither an endorsement nor a condemnation of the computer codes used to implement the mathematical models.

## MODEL DEVELOPMENT

All models for the behaviour of jointed rock considered in this study are based on the commonly accepted 'stack-of-bricks' conceptual model. This model assumes that the jointed rock mass consists of intact-rock 'bricks' surrounded by interfaces on all sides that allow the bricks to move relative to each other. The 'stack-of-bricks' conceptual model contrasts with the 'effective continuum' model in which the jointed rock mass is modelled as a continuum whose strength and stiffness are degraded from the intact-rock values based on the spacing and orientation of the joints.

The computer models investigated in the study incorporated the 'stack-of-bricks' conceptual model for jointed rock using the five distinct approaches: the DIBS code used the discrete element method with rigid elements,<sup>19</sup> the UDEC code used the discrete element method with deformable elements,<sup>20</sup> the EXCALIBUR code used the finite element method with joint elements,<sup>21</sup> the FLEX code used the finite element method with compliant slidelines<sup>22</sup> and the PRONTO code used the finite element method with non-compliant slidelines.<sup>23</sup> The computer models were developed and executed by people who are knowledgeable in the mechanics of jointed rock, and who have experience with the computer codes used to implement the models.

Participants for this study were selected based on their knowledge of mathematical models for dynamics of jointed rock and their in-depth familiarity with the computer code used. These qualifications assured knowledgeable and rational development of the mathematical models and efficient, accurate implementation of the models in the computer codes. Also, in-depth familiarity with the computer code used in the program was valuable because it allowed the user to find and fix algorithmic errors that were uncovered in the course of the program.

### *Step 1: Benchmarking*

Model development followed a sequence of five steps in which the models were tested and revised. The first step comprised a benchmark calculational activity<sup>24,25</sup> to verify the models and to show the influence of the mathematical model on the predicted response of a tunnel in jointed rock. The benchmarking approach taken was to solve five increasingly complex problems for which the material behaviour, domain, boundary conditions and initial conditions were

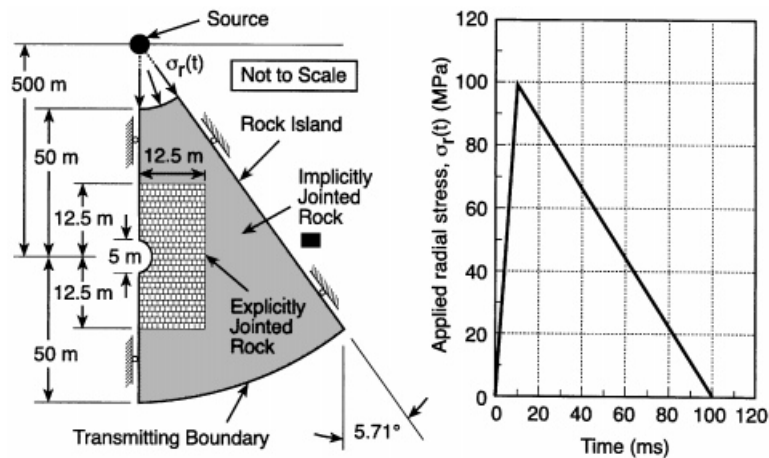


Figure 1. Geometry and loading for the primary benchmark problem

completely specified. The computer solutions for each problem were compared with analytical solutions, when possible, and with each other when no analytical solution could be obtained. The first three problems in the sequence investigated the static response of the intact material and the normal and shear behaviour of the joints. The fourth problem assessed wave propagation in the jointed rock mass. The final problem involved dynamic loading of a lined tunnel in a jointed rock mass by a cylindrically divergent stress wave, as shown in Figure 1.

Results of each problem were compared before the next problem was attempted, and differences in calculated outputs were studied to determine the cause. This methodical procedure revealed coding errors and algorithm deficiencies that were corrected. However, it also revealed fundamental differences in model behaviours and predictions that could be traced to model formulation and the method for incorporation of the 'stack-of-bricks' conceptual model.

Figure 2 shows tunnel-closure results from the final benchmark problem, dynamic loading of a lined circular tunnel in jointed rock. Three models produce similar tunnel deformation suggesting that three approaches; discrete elements with deformable elements (UDEC), finite elements with joint elements (EXCALIBUR) and finite elements with compliant slidelines (FLEX), produce adequate results for this class of problem. The study revealed unacceptable approximations of the relevant mechanics in the discrete element method that used rigid elements and the finite element method that used non-compliant slidelines. The study also showed the difficulty in solving large problems involving significant non-linear material behaviour, especially without solving a sequence of simple problems to discover computer code errors and the implications of modelling assumptions.

### Step 2: Parametric study

The next step in model development was to carry out a parametric study to investigate the importance of selected variables on tunnel closure, and how the importance of these variables differed with location within the parameter space.<sup>26</sup> The study was designed using a complete

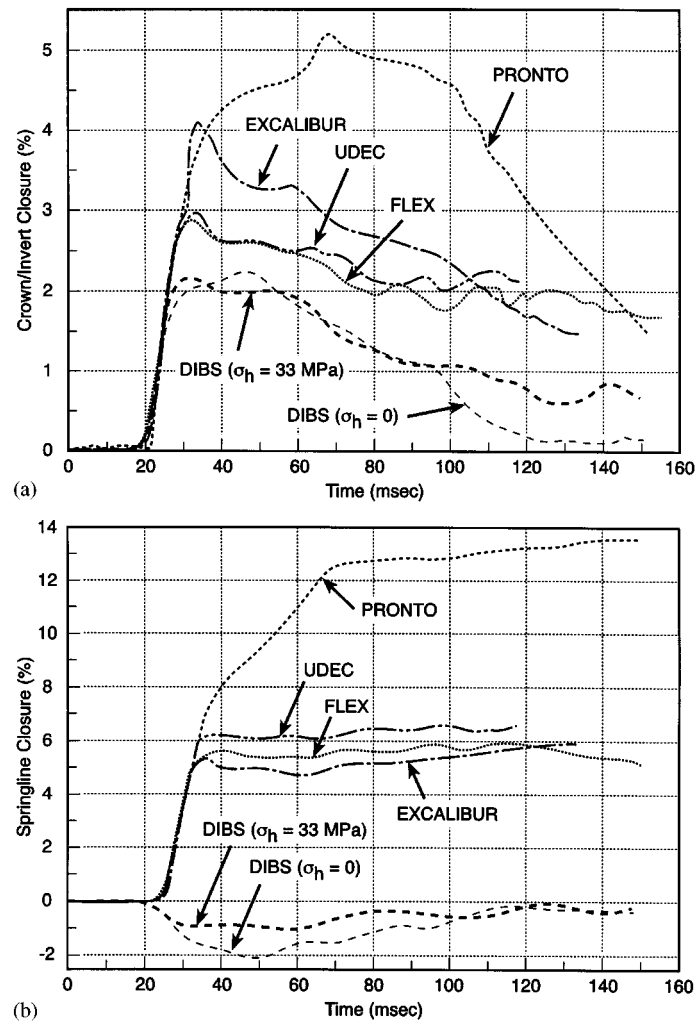


Figure 2. Comparison of calculated tunnel closures in the benchmark study: (a) Crown-invert closure; (b) springline closure

two-level factorial design for nine variables, resulting in 512 individual calculations. For simplicity, the scope was limited to simulations of dynamic loading of circular tunnels in intact rock using only two computer models, EXCALIBUR and FLEX. The problems solved had a geometry similar to that for the primary benchmark problem shown in Figure 1. The nine variables studied were: range from the loading source, peak incident stress, dilation during inelastic deformation of the rock duration of the positive phase of the loading wave, initial position of the cap in the Sandler–Rubin<sup>27</sup> cap model, ratio of rock strength in triaxial extension to that in triaxial compression for a three-stress-invariant formulation of the Sandler–Robin cap model, diameter of the tunnel, divergence of the loading wavefront and computer model.

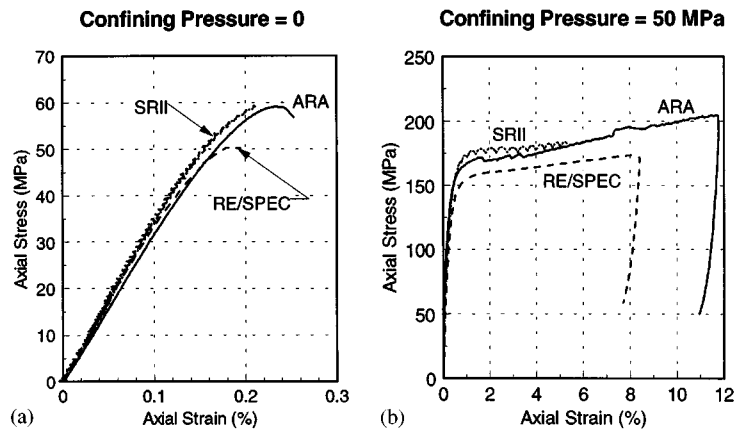


Figure 3. Stress-strain curves for Salem limestone: (a) Unconfined compression; (b) triaxial compression

Results showed the three most important variables to be the peak stress, the ratio of rock strength in extension to that in compression and the degree of dilatancy assumed for inelastic deformation. Surprisingly, the fourth most important variable was the computer model, in spite of the effort to reduce differences among models in the benchmark activity. Sensitivity to the computer model was traced to spatial discretization and the computer codes. Additionally, the results showed that the importance of variables depended on the location in the parameter space, which was indicated by the large two-factor and three factor interactions. This result is not surprising, but is important because it shows that verification and validation of a computer model in one region of the parameter space may not be sufficient to obtain accurate results in other regions.

### Step 3: Constitutive models

The third step in development of models for structural deformation in jointed rock was to develop constitutive models for the rock to be used in the predictions of tests performed for computer model development and model validation. The rock chosen for these tests, a porous limestone from the Salem formation near Bedford IN, is the same rock used in the jointed-rock precision test mentioned earlier.

A comprehensive laboratory-testing program was conducted on Salem limestone to determine its constitutive parameters.<sup>28–31</sup> Intact specimens were tested in triaxial compression and triaxial extension to determine the parameters in a three-invariant formulation of a cap model<sup>27</sup> that is commonly used to describe the behaviour of soil and porous rock. The data showed little scatter in either strength or the stress–strain curves, and the results were reproducible among three laboratories, as shown in Figure 3. This figure also shows that Salem limestone is brittle in unconfined compression, but is fairly ductile at low confining pressure. The brittle-to-ductile transition occurs at a confining pressure of about 35 MPa. The data show that the rate of strain hardening increases with increasing confining pressure.

Figure 4 shows strength data from triaxial compression and triaxial extension tests.<sup>30</sup> The solid line is a fit to the compression data, while the dashed line through the extension data is based on

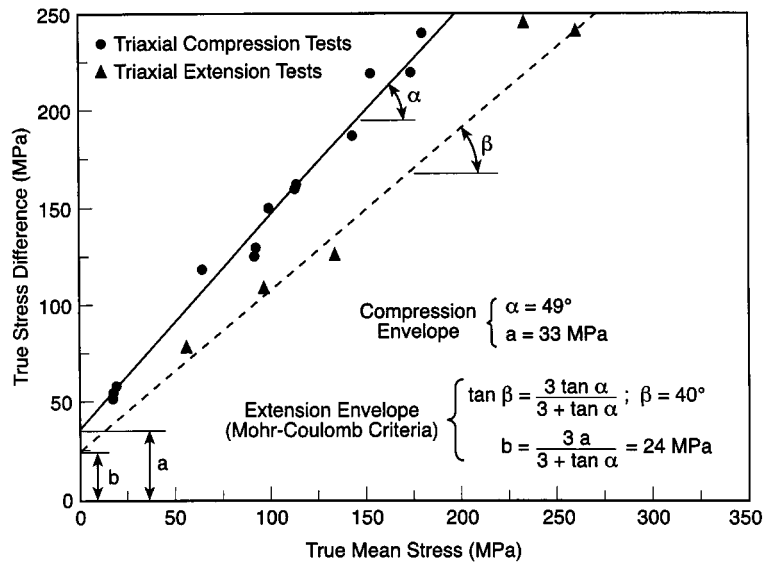


Figure 4. Comparison of extension and compression strength envelopes for Salm limestone

the Mohr–Coulomb model using the parameters determined by the fit through the compression data. The good agreement between the predicted strength in extension, shown by the dashed line, and the extension strength data show that the Mohr–Coulomb model accurately predicts the ratio of strength in extension to that in compression, and that the failure criterion for Salem limestone depends on all three stress invariants. This is an important observation because the parametric study identified the ratio of strength in extension to that in compression as an important variable.

Tests were also conducted on joints to determine their strength and stiffness.<sup>30</sup> Special specimen preparation procedures were employed to ensure that the joint surfaces in the laboratory tests were similar to those in the jointed-rock precision test. The normal compressibility of the joint surfaces was determined by unconfined compression tests on specimens with a single joint oriented at 90° to the specimen axis. Each specimen was loaded to approximately 75% of its unconfined strength and then unloaded. Figure 5(a) shows typical joint compressibility data. Under normal loading, the joints are fully closed after approximately 0.05 mm displacement.

The shear strength of the joints was determined by a series of triaxial compression tests on cylindrical specimens, each containing a single joint oriented at 30° to the specimen axis. The confining pressure in these tests ranged from 1 to 35 MPa. At confining pressures up to 30 MPa, the specimens failed by sliding of the joints at approximately constant stress. When loaded at 35 MPa confining pressure the intact portion of the test specimen failed without sliding along the joint. Figure 5(b) plots peak shear stress on the joint as a function of normal stress on the joint for tests performed at confining pressures up to 30 MPa. The joint strength data are well represented by a straight line passing through the origin with a 38.3° friction angle.

Tests were also performed to determine the rate dependence of the compressive strength. Triaxial compression tests were performed at a confining pressure of 25 MPa and at axial strain

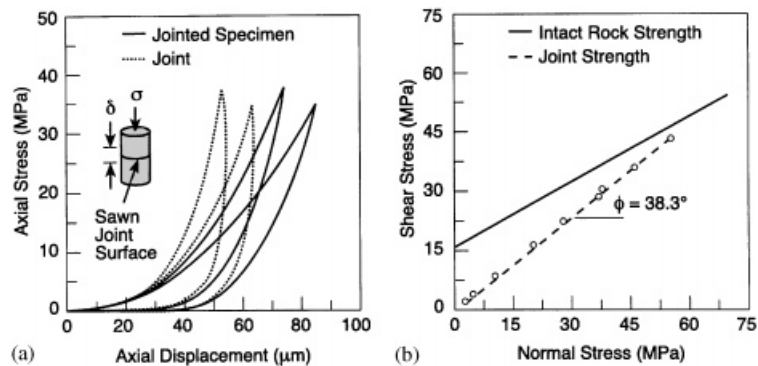


Figure 5. Compressibility and strength of joints in Salem limestone: (a) Compressibility; (b) strength

rates between  $10^{-5}$  and  $10^{-2} \text{ s}^{-1}$ .<sup>29</sup> Results show that the strength increases linearly with the logarithm of strain rate at about 5 percent per decade.

The comprehensive, high-quality data allowed the constitutive models to be calibrated to both intact rock and joint behaviour. This is an important step when computer model predictions are to be compared with measurements from experiments.

#### Step 4: Precision tests

The fourth step in model development was to perform precision tests on specimens of intact rocks containing circular tunnels. Both static and dynamic precision tests were carried out to produce data on the deformation of a circular tunnel in intact Salem limestone. Three static tests<sup>31</sup> were performed on limestone cylinders that were 305 mm in diameter and 457 mm high. A 20-mm-diameter circular tunnel was drilled at specimen midheight. In one test, the tunnel was unlined and in the other two tests it was lined with a fully annealed 3003 aluminum tube having a 0.9-mm-thick wall. The specimens were placed in a large triaxial compression apparatus<sup>32</sup> and slowly loaded with a load history in which both the axial load and confining pressure were increased. Deformation of the tunnel crown-invert and springline diameters and also axial and circumferential strain at several locations on the surface of the limestone cylinder were measured throughout the test. Figure 6 shows the specimen geometry and a typical load history for these precision tests.

The static tests were the first of the precision tests to be performed. They were also the least precise. For example, there were no repeated measurements to determine the precision of the data. In fact, for one test in which the pressure loading followed the shear failure surface for part of the history, attempted repeats resulted in the specimen fracturing, as might the specimen in a triaxial compression test. Also, the strain gages mounted on the surface of the limestone produced scattered and erratic records, which were not very useful for model development.

Two dynamic precision tests<sup>33,34</sup> were performed on large limestone blocks. Test specimens were octagonal cylinders 1.67 m high and 1.2 m in diameter, as shown in Figure 7. The test specimen contained up to five tunnels having the same diameter and aluminum liner as in the static tests. A spherical cavity at the centre of the specimens was filled with a 111-g charge of



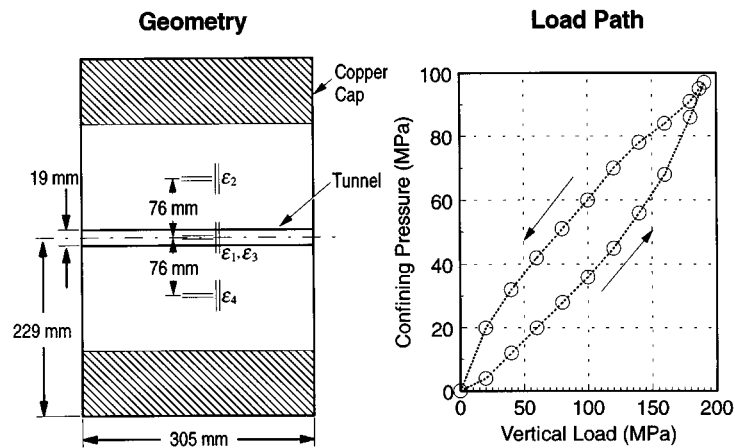


Figure 6. Specimen geometry and typical load history for static precision test on intact limestone

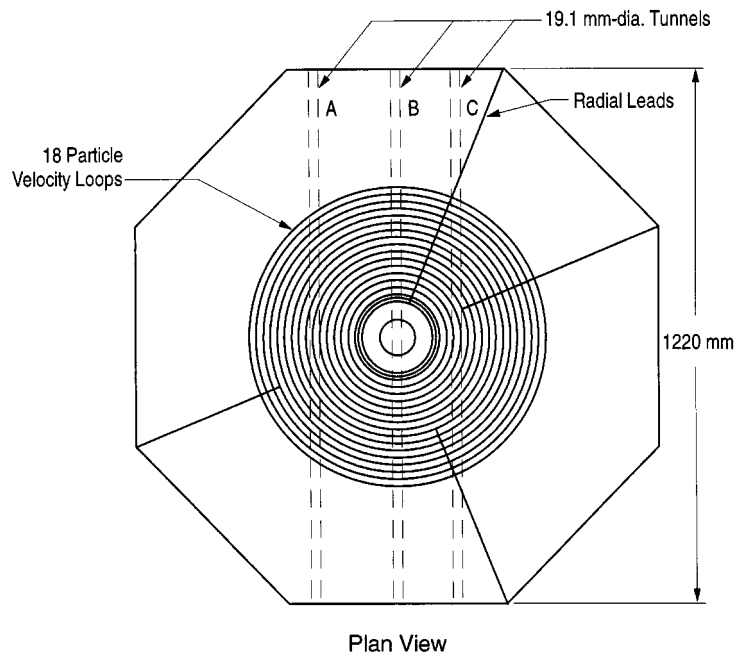


Figure 7. Specimen geometry for dynamic precision tests on intact limestone

pentaerythritol tetranitrate (PETN). The test specimen comprised a top and bottom half to allow loading of the explosive charge and to permit instrumentation of the rock. Radial particle velocity was measured by wire loops in the plane of the interface between the top and bottom halves of the specimen. During the test, a magnetic field was applied to the specimen so that the moving wires

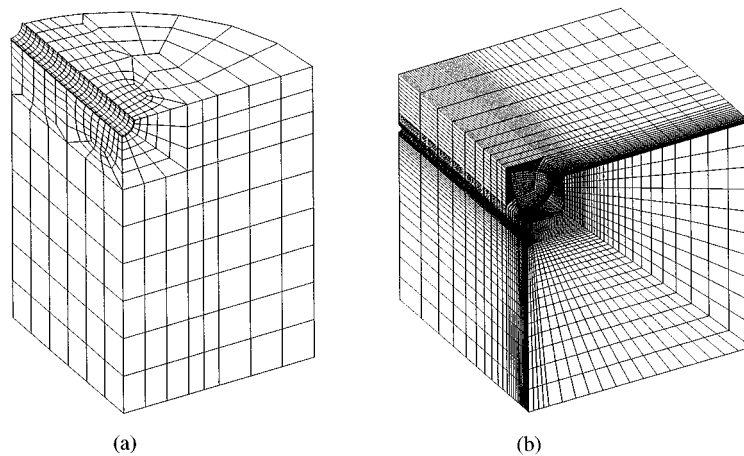


Figure 8. Meshes used for the static and dynamic analyses: (a) Static analysis; (b) dynamic analysis

generated a current proportional to the particle velocity. Stress gages were also installed at several ranges to measure the normal stress history in the radial direction. The tunnels were instrumented to measure the deformation history of the crown-invert and springline diameters, where the crown-invert diameter is defined to be in the direction of wave propagation, e.g. radial from the spherical charge. The dynamic tests were repeated tests and showed good repeatability. Particle velocity, tunnel-closure and stress data were measured at several ranges from the explosive charge and were available to be simulated by the models.

#### *Step 5: Model predictions for intact rock*

The fifth and final step in model development was to compare model predictions for structural deformation in intact rock with data from the precision tests. Three-dimensional models were constructed to model the tests. Mesh-refinement studies performed to determine the necessary spatial discretization, however, were done with two-dimensional models. Figure 8 shows typical meshes used for the static and dynamic analyses. Each mesh take advantage of the symmetry in the problem to reduce the size of the model. The mesh for static analyses, shown in Figure 8(a) contained about 1000 elements and model only one octant of the test specimen: planes passing through the tunnel mid-length, crown-invert and springlines are symmetry planes. The mesh for dynamic analysis, shown in Figure 8(b) contained about 50,000 elements. The dynamic mesh is much larger than the static mesh for two reasons. First, extremely small elements are required to provide the fine spatial discretization needed to prevent significant numerical attenuation of the stress wave between the mesh boundary and the tunnel. Second, the larger specimen in the dynamic tests must modelled to prevent spurious reflections of the stress wave.

For both the static and dynamic cases, the numerical simulations were completed before the experimental data were made available to the modellers. After comparison with the experiments, the models were refined to improve agreement with the measurements. This sequence is essential because it is well known that a priori knowledge of the experimental results allows the simulation

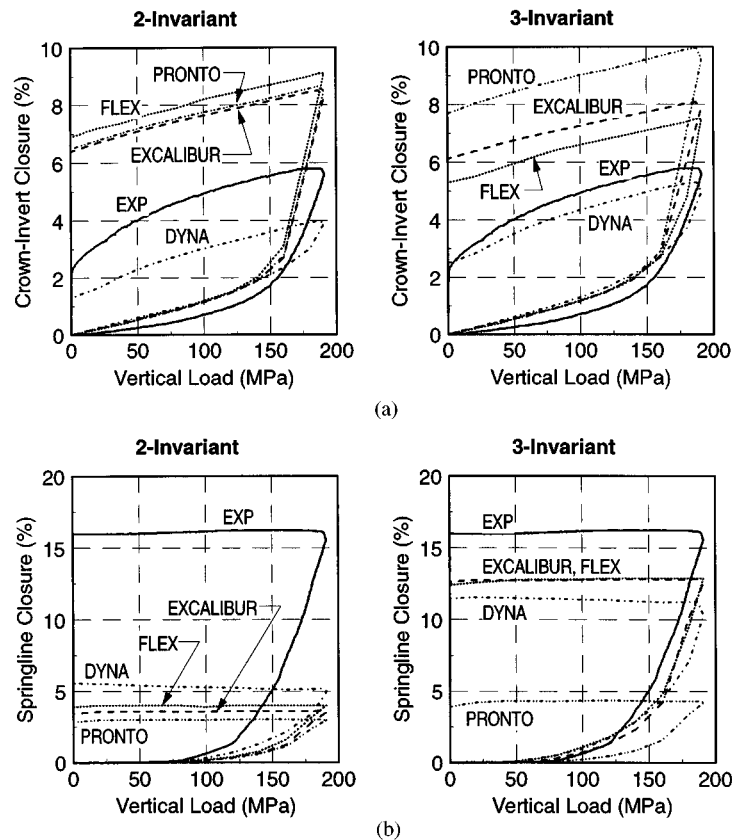


Figure 9. Measured and predicted crown-invert and springline tunnel closures for a static test: (a) Crown-invert closure; (b) springline closure

to match the measurements quite well. The model results presented here are from the pre-test predictions. Outputs from the refined models match the measurements much better.

A new computer model was added to the program for intact rock calculations. DYNA<sup>35</sup> was added to replace UDEC, which is not designed to address three-dimensional problems. The three-dimensional successor to UDEC was not used because it had not been modified to incorporate the results of the previous parts of the program.

Figure 9 plots measured and predicted deformations of the tunnel crown-invert and springline diameters for the static test with the unlined tunnel. The loading for this test is that shown in Figure 6. To show the effect of the ratio of strength in triaxial extension to that in triaxial compression, the tests were first calculated with a two-invariant cap model and then with a three-invariant cap model. The two-invariant models matched the measured triaxial compression strength data shown in Figure 4. The three-invariant models matched both the triaxial compression and extension data shown in the figure, with a smooth decrease in shear strength as the stress state moves from compression to extension.

The two-invariant models were identical in all codes, except DYNA, which used a single-surface, smooth-cap approximation<sup>36,37</sup> of the two-surface Sandler–Rubin cap. The three-invariant cap models, however were different in each model: DYNA used a formulation based on the work of Rubin,<sup>38</sup> EXCALIBUR used the formulation of Willam–Warnke,<sup>39,40</sup> FLEX used a modification of the Willam–Warnke formulation<sup>41</sup> and PRONTO used an even different formulation.<sup>42</sup>

Calculations using the two-invariant models predict similar tunnel deformation, with the exception of the DYNA predictions, which used the smooth cap approximation. This shows that models with identical formulations for the constitutive behavior produce essentially the same answer. The difference among predictions is consistent with the results of the parametric study, which shows that computational model itself is a significant variable in simulations. Figure 9 clearly shows however, that generally accepted derivations from the prescribed constitutive behaviour can produce noticeable differences in results, as shown by the DYNA predictions. Finally, although the predictions agree with each other, they do not match the measurements well.

Predictions using the three-invariant models scatter more than the two-invariant predictions, but give better agreement with the data. The scatter in predictions results from the different three-invariant formulations used in the individual models. However, better agreement with the measurements shows the need to incorporate this aspect of material behaviour, which was shown in Figure 4. This is consistent with the findings of the parametric study, which showed that the ratio of rock strength in extension to that in compression is an important variable in the models. Analysis of the stress history at several locations around the tunnel shows that the stress paths are not radial and vary from point to point so that it is not feasible to calibrate a two-invariant model to the test results.

Results of predictions for the other two static tests are similar, but less dramatic because the tunnel deformations were only about twenty per cent as large as those shown in Figure 9. Predictions using the two-invariant models always under-predicted the springline closures; however, predictions using the three-invariant models sometimes under-predicted and sometimes over-predicted the measurements. The models showed a consistent trend in predictions of the three tests: DYNA usually predicted the largest springline deformation (the right-hand side of Figure 9(b) is a minor exception), and PRONTO always predicted the smallest. Also, the PRONTO predictions were the least sensitive to using the two- or three-invariant constitutive model.

The strain rates in the dynamic tests are much larger than those imposed in the laboratory tests described earlier that showed that the strength increases linearly with the logarithm of strain rate at a rate of nearly 5 per cent per decade. There is significant data for a range of materials, including rocks like limestone, showing that at high strain rate, strength increases much more rapidly with strain rate the linear dependence on the logarithm of strain rate found in lower rate tests.<sup>43</sup> Since no high-strain-rate data were obtained from the laboratory testing carried out for this program, the rate-dependent models were fitted to the particle velocity data from the dynamic tests. Figure 10 shows the measurements and predictions of particle velocity at two ranges using rate-independent and rate-dependent models. The repeatability of the measurements shows that the experiments provide good precision data for model validation.

The rate-independent models accurately predicted arrival times, loading slope and both positive and negative phase duration fairly well. However, the peaks of the waveforms were truncated. The fitted, rate-dependent models also match the peak velocities in addition to the other wave characteristics.

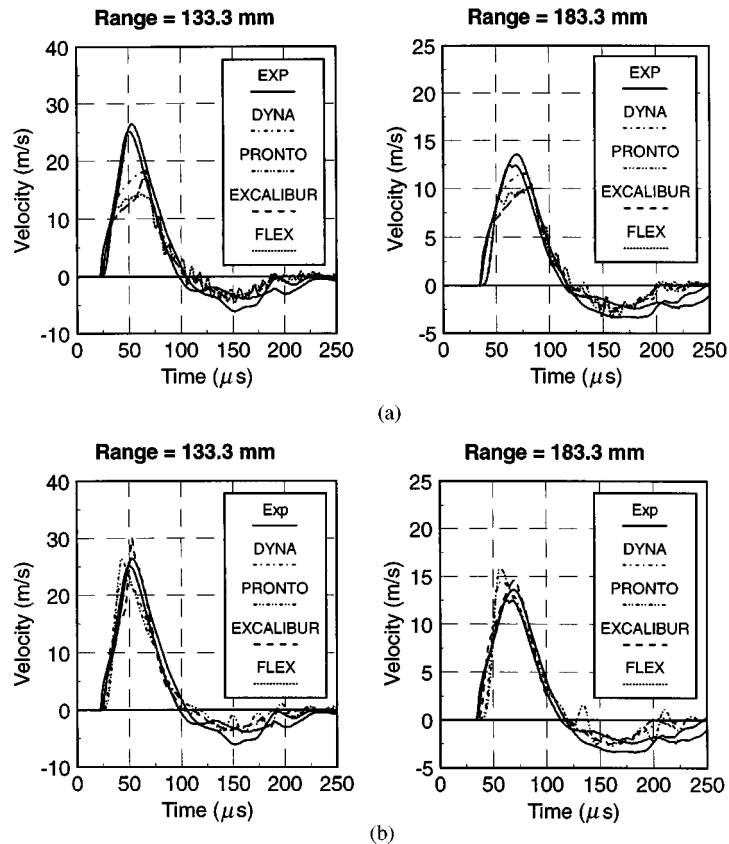


Figure 10. Measured and predicted particle velocity histories for the dynamic tests: (a) Rate-independent models; (b) rate-dependent models

Rate dependence was incorporated in EXCALIBUR through a linear relationship between strength and the logarithm of strain rate, but with different parameters than found in the low-rate laboratory testing. The other three models incorporated rate dependence using the formulation of Duvault and Lions,<sup>44</sup> which is a linear overstress model.

Figure 11 plots the predicted and measured radial stress at two ranges. As was found for particle velocity, the rate-dependent models make more accurate predictions of the peak stress than do the rate-independent models. The improvement is especially significant at the closer range, 145 mm, where the stress and strain rates are high. The improved predictions of the radial stress component show the importance of adopting a rate-dependent formulation.

Figure 12 and 13 plot measured and predicted deformation of the crown-invert and springline diameters at the same two ranges for which Figure 11 showed the stress. As was the case for stress and particle velocity, the measurements show very good repeatability. The rate-dependent models predict the crown-invert deformation somewhat more accurately than do the rate-independent models, as expected. However, the rate-dependent models make surprisingly poor predictions of the springline deformations. In fact, the rate dependent DYNA and PRONTO

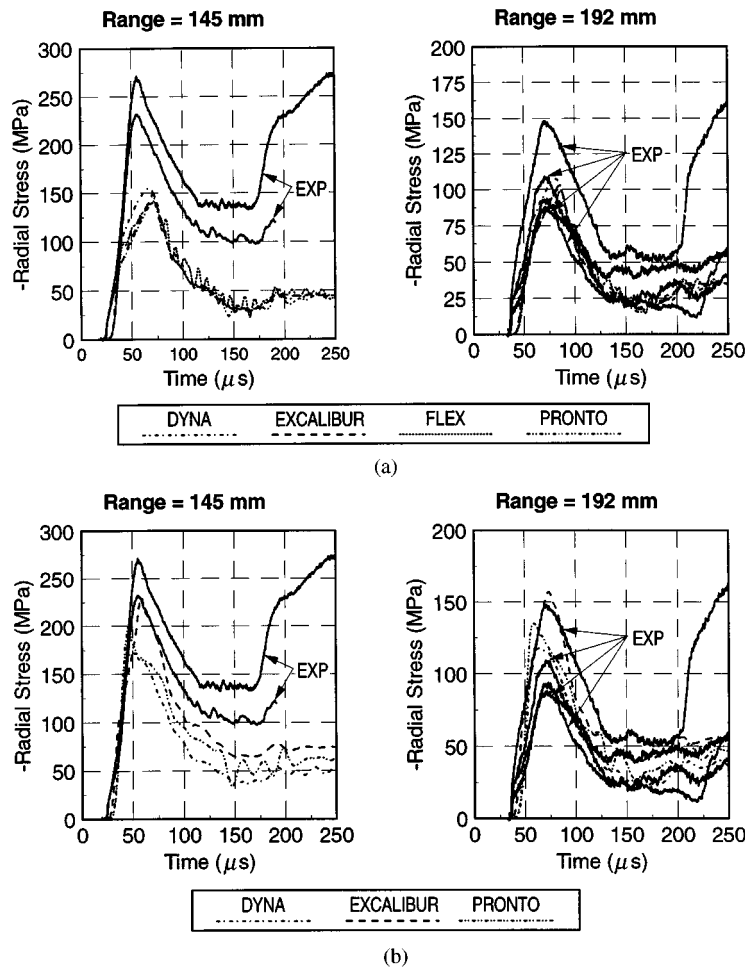


Figure 11. Measured and predicted stress histories for the dynamic tests: (a) Rate-independent models; (b) rate-dependent models

models do not even predict the correct sign. This shows that although it is clear that rate-dependent models are needed to predict the stress, particle velocity and crown-invert closure, the functional form used to incorporate rate dependence in the constitutive models is very important for predicting all aspects of tunnel deformation.

Predictions of the measurements made in the tests on intact limestone revealed some shortfalls in the models and prompted revisions and addition of new features such as three-invariant and rate-dependent constitutive models. The dynamic tests were more useful in this step than were the static tests. This is primarily because the dynamic tests provided a wider range of measurements and because they had a known level of precision resulting from the repeated measurements.

The five-step model-development phase concluded with additional features added to the models that were believed to improve predictions further. The most significant new feature was

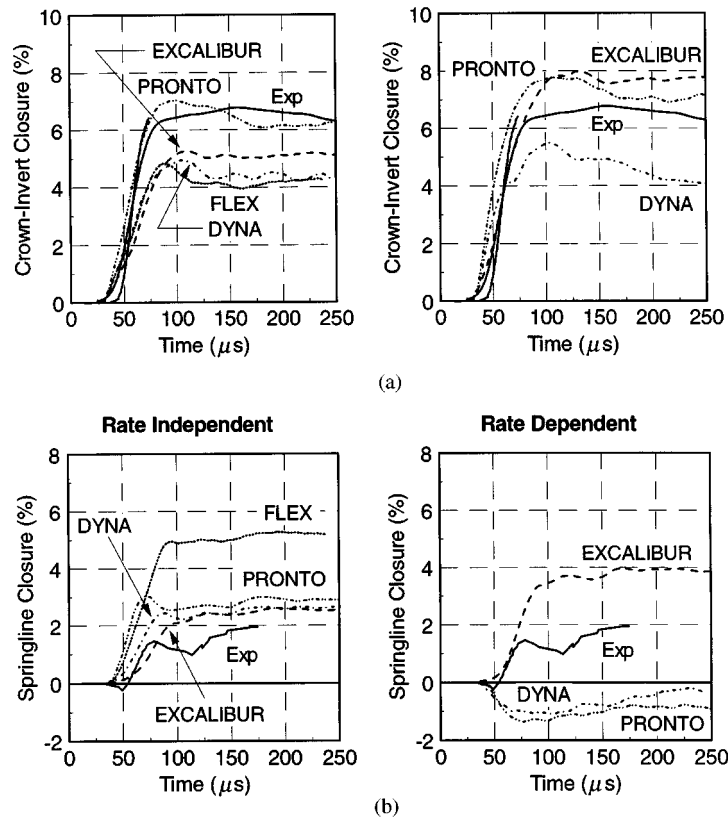


Figure 12. Measured and predicted crown-invert and springline tunnel closures for the dynamic tests at a range of 145 mm; (a) Crown-invert closure; (b) springline closure

the addition of a damage mechanism to the intact rock constitutive models. Damage was incorporated primarily to simulate the post-peak degradation of strength with inelastic deformation and to model the formation of macroscopic fractures.

## VALIDATION

Model validation comprised two steps. First, a jointed-rock precision test<sup>17,18</sup> was performed to provide data to validate the computer models, as described earlier. The test had geometry and loading similar to the primary benchmark problem shown in Figure 1. The test incorporated the 'stack-of-bricks' conceptual model for jointed rock masses.

The jointed-rock test specimen was made of over 4000 limestone bricks, with each brick nominally 51 mm square and either 0.6 or 1.2 m long. The bricks were stacked into a nearly cubic rectangular prism 2.1 m square and 2.4 m long with a central 0.4-m-diameter circular hole lined with a thin aluminum tube. Figure 14 shows the geometry of the test specimen. The figure also shows the location of the 46 gauges mounted in the midplane of the specimen to measure particle velocity, stress, joint slip and tunnel closure.

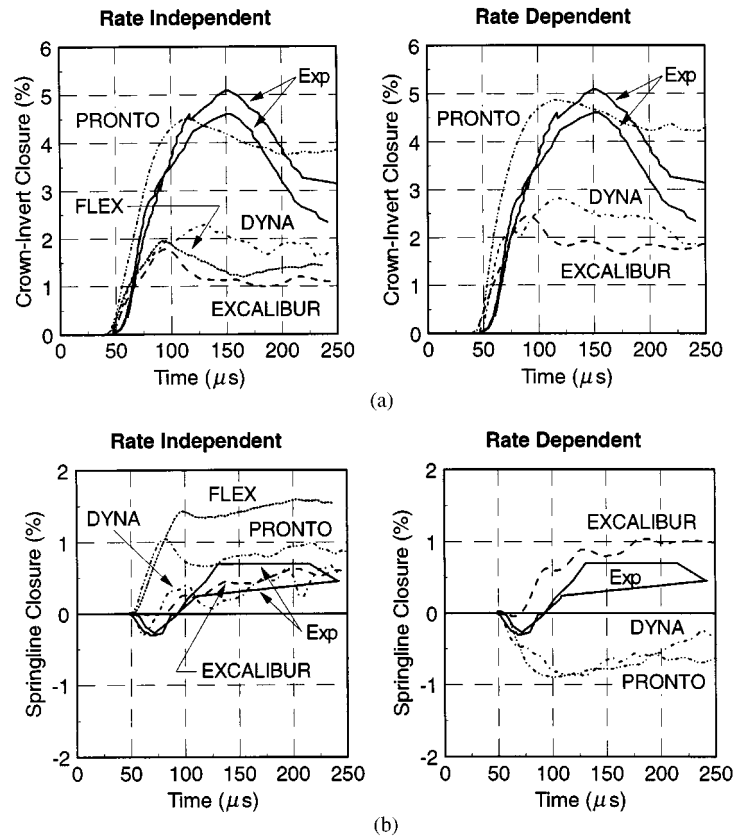


Figure 13. Measured and predicted crown-invert and springline tunnel closures for the dynamic tests at a range of 192 mm: (a) Crown-invert closure; (b) springline closure

The jointed limestone cube was placed in a deep pit that was later filled with concrete. The top surface of the concrete tested was formed to include a cylindrical section. The entire top surface of the concrete pit was covered with explosives that were detonated to produce a cylindrically diverging stress wave. The stress wave at the depth of the top of the cube had a radius of 4.4 m, a rise time of about 500  $\mu$ s, a peak stress of about 100 MPa, a peak particle velocity of about 14 m/s, a total radial displacement of about 25 mm, and peak circumferential strain of about 0.6%. This divergent dynamic environment was sufficient to exercise intact rock comminution, joint slip, intact rock fracture, and permanent deformation of the lined opening.

For the second validation step, models were selected to predict the results of the jointed-rock precision test: the finite element codes EXCALIBUR and FLEX and the discrete element code UDEC. The constitutive model for intact limestone used in EXCALIBUR is a coupled elastic-plastic-damage formulation<sup>45</sup> involving the following mechanisms: strain-hardening three-invariant cap<sup>27,46</sup> for crush strength with associated plastic flow; perfectly-plastic limit (cap) for tensile strength; perfectly-plastic three-invariant failure surface<sup>39,40</sup> for shear strength with fully associated flow in triaxial compression, transitioning to non-associated flow with half the dilatancy of



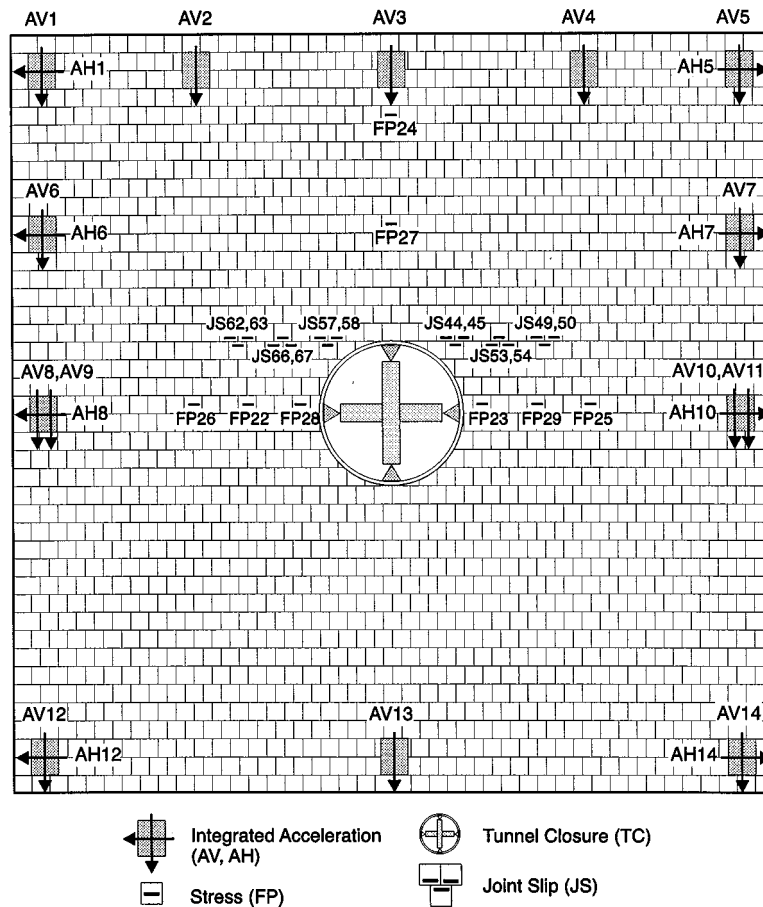


Figure 14. Geometry for the large jointed-rock precision test

associated flow in triaxial extension;<sup>47</sup> coupled elastic-plastic modulus reduction<sup>48</sup> for damage-induced softening; implicit oriented strain localization<sup>49</sup> for fracture; and strain-rate effects on strength and fracture energy.<sup>50</sup> The model for joints involved an interface element<sup>51</sup> with constant shear stiffness, non-linear normal stiffness variation with closure based on the benchmark joint stiffness equation<sup>24,25</sup> and the data in Figure 5 and non-dilatant Coulomb friction rule with  $\phi = 38.3^\circ$  which allows stick, slip and separation. The constitutive model for the aluminium liner was an isotropic-hardening Mises model.

The intact-limestone constitutive model used in FLEX employs an elastic-plastic softening formulation with a three-invariant strain-hardening cap, a  $J_1$  tension surface for tensile strength, a three-invariant failure surface for shear strength,<sup>41</sup> a non-associated flow rule with half the dilatancy of associated flow, isotropic softening implemented by shifting the failure surface and tension limit along the  $J_1$  axis with increasing dilatant volumetric strain and allowing the stresses to relax with a damaged viscosity,<sup>52</sup> and the Duvault–Lion rate-enhancement algorithm<sup>44</sup> for

both the cap and the shear surface. The joint model which allowed contact, separation and sliding was based upon a penalty spring slideline algorithm.<sup>53</sup> The normal joint stiffness was a piecewise linear elastic model based upon the data shown in Figure 5. The joint shear behaviour is represented by a constant stiffness and a Coulomb failure surface ( $\phi = 38.3^\circ$ ). The constitutive model for the aluminium liner was an isotropic-hardening Mises model.

The constitutive model for intact limestone used in the UDEC code is an elastic-plastic softening model with no cap, a tension cut-off, a Mohr–Coulomb failure surface for shear strength, non-associated flow with zero dilatancy,<sup>54</sup> associated flow in tension, isotropic softening of the cohesion and tensile strength and no rate dependence. The joint model was a Coulomb slip model with a constant shear stiffness and a non-linear normal stiffness based on the data shown in Figure 5. The constitutive model for the aluminium liner was an isotropic-hardening Tresca model.

The models developed for this validation effort have noticeably different constitutive models for the intact rock. These differences result from the limitations of the computer codes and the difference in experience and insight of each of the modellers. The constitutive behaviour of the joints is similar, although the algorithm for incorporating the ‘stack of bricks’ conceptual model is different for each model, as pointed out earlier.

The computer models incorporated information about the effective vertical and horizontal gaps between the limestone bricks in the experiment. The thicknesses of these gaps were determined using an indirect technique that relied on careful measurements of the overall dimensions of the stack in both directions. The contribution of the solid material to these measurements (i.e., the values that would be expected in the absence of gaps) was estimated by multiplying the number of bricks by the average brick thickness. The differences between these numbers and the actual measurements then provided an estimate of the total effective gap thickness. Dividing these differences by the number of joints then provides an estimate of the average effective gap thickness in each direction.

Post-test measurements of the test specimen showed that the deformation was symmetric about a vertical plane through the tunnel midlength and was nearly constant in the middle half of the specimen, with slight end effects observed in both of the end quarters. Therefore, the computer models used two-dimensional, plane-strain formulations. Taking advantage of the symmetry about the vertical plane passing through the tunnel crown and invert allows further simplification.

The models used the measured particle velocity as the time-dependent boundary condition that loaded the domain. In general, it is difficult to prescribe boundary conditions so close to the tunnel in a problem such as this because of the perturbation to the stress and velocity fields caused by the tunnel. However the boundary conditions in this case include the perturbation because the boundary conditions were measured in the test rather than inferred from test data or calculations of ground motion that do not include a tunnel. Particle velocity was chosen for the boundary condition in this test for two reasons. The first is that measurements of the two non-zero components of particle velocity can be made more reliably than can measurements of the two non-zero components of traction. The second reason is that if the load reaches the rock strength over large portions of the test specimen, traction boundary conditions allow development of an unrealistic collapse mechanism. Velocity boundary conditions, however, prohibit this mechanism by correctly accounting for the inertia of the mass surrounding the test specimen.

The models predicted measurements made during the test at the gauge locations shown in Figure 14: the stress history measured at two locations above the crown and at three locations

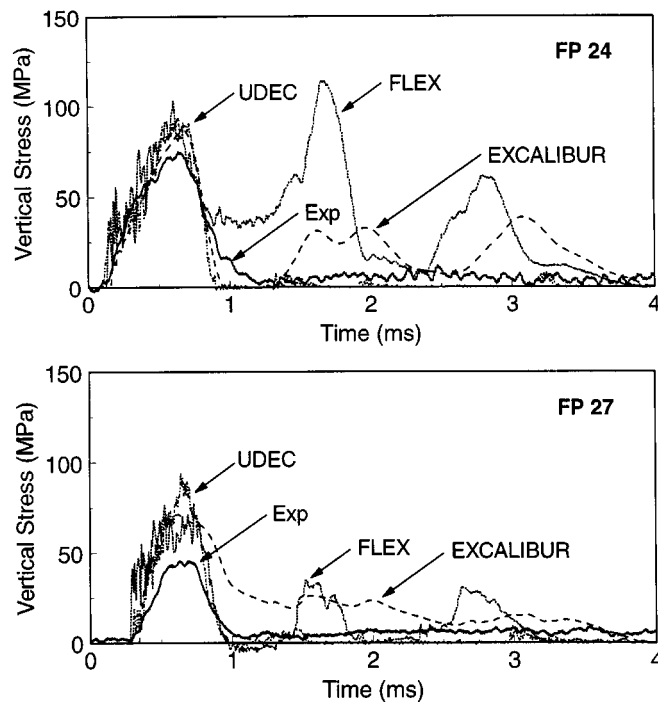


Figure 15. Predicted and measured stresses on the specimen centreline above the tunnel crown

laterally from the springlines, deformation of the tunnel crown-invert and springline diameters, and joint slip at three locations located laterally from near the top of the tunnel. The models also predicted the post-test deformed shape of the aluminium tunnel linear and the post-test deformation and damage in the jointed limestone.

Figure 15 shows the predicted and measured stresses at the two gauges located on the specimen centreline above the tunnel crown. Unfortunately, because these gauges were located on the specimen centreline, it was not possible to make comparable measurements, so it is not possible to ascertain the precision in the measurements. All models predicted the arrival time accurately at both gauges. Also, all models accurately predicted the peak stress, about 100 MPa at the upper gauge. However, at the lower gauge, the measured peak is only about sixty per cent of the predictions. At both gauge stations, FLEX predicts large second and third pulses, suggesting that there are spurious reflections somewhere in the model.

Figure 16 shows the predicted and measured stresses at the three gauges located adjacent to the springlines. Because of symmetry in the experiment, the gauges on each side of the tunnel measure similar stress histories, and therefore provide a measure of precision. As the figure shows, the precision in these stress measurements is very good. The models predict the wave arrival time accurately at all stations. Both EXCALIBUR and FLEX consistently over predict the pulse amplitude and duration, and therefore the amount of impulse in the wave. The UDEC prediction tracks the measurements quite well, with a peculiar drop to zero stress around 2 ms, which persists for about 0.5 ms.

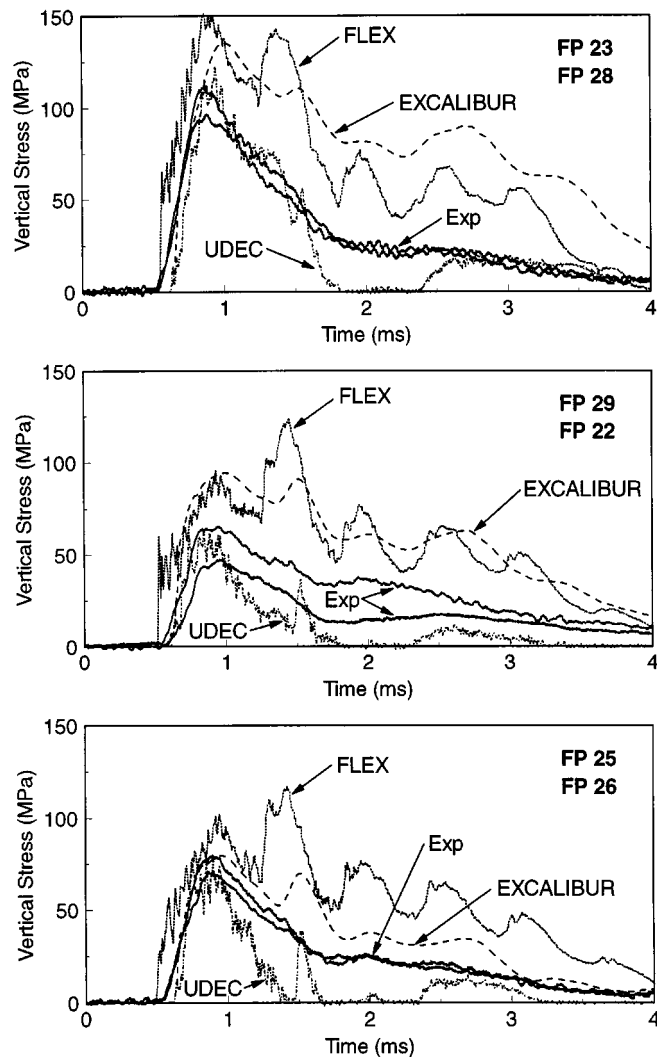


Figure 16. Predicted and measured stresses adjacent to the tunnel springlines

Figure 17 shows the predicted closures of the crown-invert and springline diameters. The gauges failed in the experiment so the measured closure history is not available for comparison with the predictions. However, the post-test measurements at the centre of the tunnel and at 0.3 m on either side of the centre are plotted on the right-hand side of the graph. All the models over predict the post-test crown-invert closure, but accurately predict the opening of the springline diameter.

The gauges for measuring slip were set to measure much more slip than was recorded in the experiment. The gauge settings were based on slip predictions in the primary benchmark

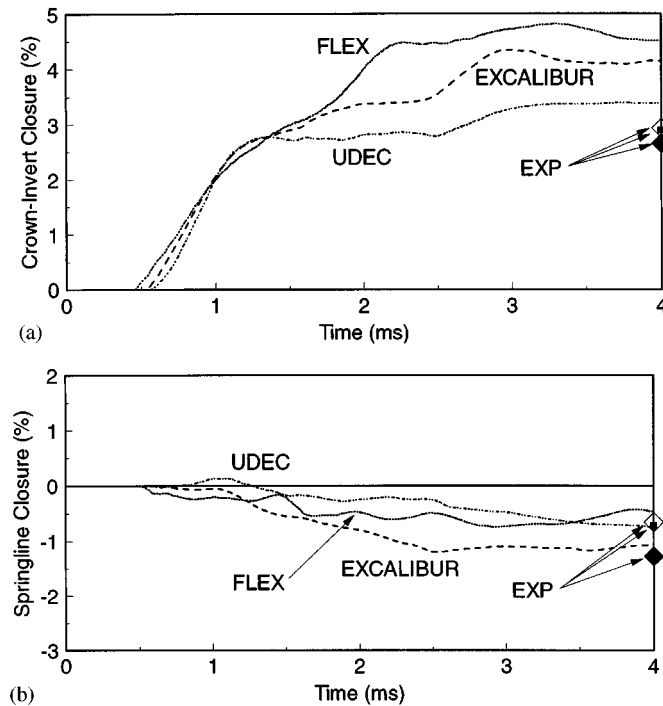


Figure 17. Predicted deformation of the crown-invert and springline tunnel diameters: (a) Crown-invert closure; (b) springline closure

problem. Measured slip was very small, and the data have very poor resolution. The model predictions were accurate in that they also predicted very small slip, approximately what was measured.

After the test, the specimen was carefully disassembled and the deformation of the stack of bricks was measured at the midpoint of the tunnel. Also, the tunnel liner was recovered and measured to determine more information than can be obtained from the crown-invert and springline diameter changes alone.

Figure 18 shows the measured and predicted shape of the deformed aluminium liner. The models generally predict the ovaled shape accurately. The FLEX prediction contains an inward bump at the invert, which was later discovered to result from an improper boundary condition for the limestone brick directly under the liner (friction was inadvertently applied between this brick and the mirror plane that was used at the vertical midplane of the region). EXCALIBUR predicts an inward bump in the liner at the crown. This deformation results from the predicted deformation of the limestone, as discussed in a following paragraph. The bumps in these two models are largely responsible for the over prediction of the crown invert closure shown in Figure 17. Except for the bumps, all three predictions match the observed liner shape remarkably well considering the differences in the models and in the predicted deformations in the surrounding bricks, suggesting that the deformed liner shape is not overly sensitive to the details of the material model that is used.

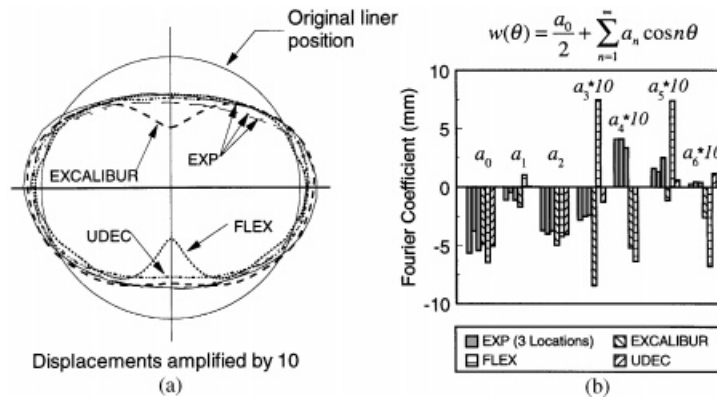


Figure 18. Measured and predicted shape of the deformed aluminium liner: (a) Deformation; (b) Fourier components

The measured and predicted liner deformations were expressed using a six-term Fourier cosine expansion, as shown in the figure. The models accurately predict that the liner deformation is dominated by the breathing ( $n = 0$ ) and the ovaling ( $n = 2$ ) modes. The relatively large first mode contributions predicted by EXCALIBUR and FLEX result from the inward bumps predicted at the crown and invert, respectively. Generally, the models do not predict the amplitudes of the higher modes well, perhaps because they are so small.

Figure 19 shows the measured and predicted deformed tunnel and surrounding limestone bricks. Post-test unstacking of the test specimen showed that the only evidence of limestone compaction was at the surface of the liner. Almost all the brick damage was in the form of splitting along the vertical midplane, typically running the entire length of the brick in the axial direction. However, this damage was concentrated around the opening. Also, unsplit bricks removed from the test article had the same dimensions as pre-test.

The observed displacement and fracture patterns were of vertical cleavage emanating upward from the springlines forming a chimney of bricks. The cleavage fractures tended to curve slightly toward each other and disappeared before reaching the top surface of the specimen. Above the springlines, the relative displacement across the cleavage planes was about 10 mm, with the bricks within the chimney moving downward relative to the rest of the test article. The cleavage planes also extended downward from the springlines, but only a few layers. In this region, the relative displacement was about 2 mm, the material outside the cleavage planes moving downward relative to the material between the cleavage planes. This deformation mechanism contrasts sharply with that found for the static and dynamic tests on intact limestone.<sup>17</sup> Post-test examination of the intact limestone shows that instead of the vertical fractures that form the chimney in the jointed specimen, intact rock gives rise to shear bands that emanate from the springlines and deviate from vertical by 25–30°.

The FLEX prediction of limestone fracturing around the tunnel and the overall deformation of the specimen is quite accurate. It gives vertical splitting of the limestone bricks and rubble (not shown) near the tunnel, just as was found in the experiment.

The EXCALIBUR prediction does not show the fracturing seen in the experiment, but gives significant ductile damage in bands that follow the fractures seen in the experiment. It also shows

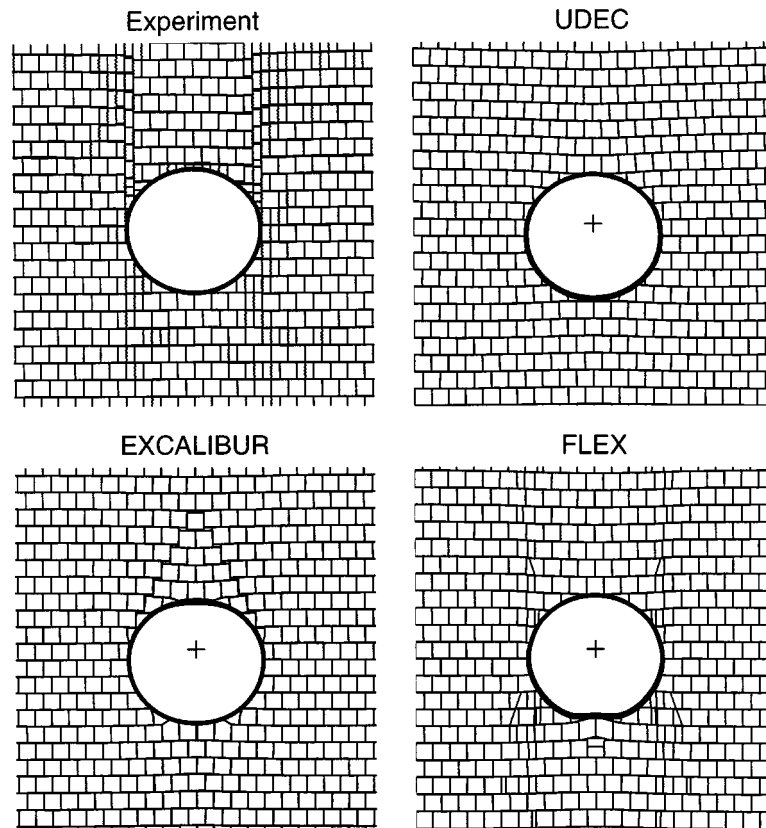


Figure 19. Measured and predicted deformations of the tunnel and surrounding limestone bricks

a wedge of limestone bricks above the tunnel that was not seen in the experiment. It is this wedge that produces the bump in the tunnel liner shown in Figure 18.

The UDEC prediction does not capture the fracturing or even give a significant concentration of any damage near the vertical fractures seen in the experiment. It shows that the damage is fairly uniformly distributed throughout the test specimen, in contrast to the measurements. Yet, it is interesting to note that while UDECs prediction of the deformation in the bricks is the least accurate of the three (see Figure 19), its prediction of the deformed liner shape is perhaps the most accurate of the three (see Figure 18).

Prediction of damage and fracturing by these models requires substantial interpretation of the model output by the modeler. Assigning physical significance to the mathematical predictions of damage is an immature capability, as shown by the results of this exercise. While the intact-rock constitutive models predict evolution of damage, determination of whether the damage has reached a level to produce a macroscopic fracture is subjective and so is the determination of whether or not the damage is brittle or ductile. While the brittle-to-ductile transition pressure has been measured in triaxial compression tests for Salem limestone, as reported earlier in the paper, calculated damage evolves around the tunnel along fairly complex load paths that are not always

above or below the measured transition pressure. Therefore, the modeller must use his judgement to discriminate between brittle and ductile fracturing based on how much and which part of the load history is above the brittle-to-ductile transition pressure.

Overall, comparison of the model predictions with the measurements was mixed. The tunnel deformation was predicted accurately. One model, FLEX, made an excellent prediction of the post-test deformation and fracturing in the limestone. EXCALIBUR showed the damage to localize near where the fractures were observed in the experiment. However, this damage was interpreted as ductile damage because of the high mean stress. Although it did not correctly predict fracturing of the intact rock, UDEC was the only model to predict the stresses accurately.

## DISCUSSION

A methodical long-term program has been carried out to develop and validate computer models for deformation of structures in jointed rock. This paper is unable to discuss all the issues and complexities addressed in the program. Some of the important issues originally arose as apparently unimportant subtleties, but turned out to have significant consequences.

The model-development program comprised a sequence of five studies starting with the benchmark study that uncovered several algorithmic and coding errors. It showed that for this class of problem both the discrete element method with deformable elements and the finite element method with either compliant slidelines or joint elements could give credible results.

The second study was the parametric study, which showed that model sensitivities vary with the problem specification and that the influence of the calculator is statistically significant, and perhaps physically significant. This is analogous to testing, where results are repeatable at two laboratories, but not reproducible between them. The parametric study also identified sensitivities that guided model refinement when comparing measured and predicted responses.

The model-development program included a comprehensive laboratory testing program to determine material properties. The Salem limestone used in the study was shown to have repeatable and reproducible material properties, and both intact rock and joint behaviour were characterized. It is important to use a low-variability and well-characterize material in precision tests so that the measurements have good precision and can be credibly predicted by the models.

The models were then used to predict the measurements from a set of static and dynamic tests performed on intact limestone. The static tests proved to be problematic for several reasons. First, the tests were not repeated so the level of precision could not be truly known. Additionally, the traction boundary conditions produced very sensitive problems when the loading was near the shear failure surface. The dynamic tests, however, produced a variety of high-precision data. Modelling of these tests showed the importance of incorporating material behaviour such as three-invariant constitutive models and rate effects, although fully satisfactory models were not developed for rate effects.

The validation portion of the program started with the jointed-rock precision test. This test was successfully executed with high precision. Finally, the computer models were used to predict the test. Predictions of the measured post-test liner deformation were very good. However, predictions of rock-mass stress, deformation and damage varied widely. This shows that sophisticated computer models for deformation of structures in jointed rock cannot universally make accurate predictions of all aspects of the problem.

This program has illustrated some important issues that apply generically to development and validation of sophisticated models for problems in engineering mechanics. First, it demonstrated



that code verification is essential to eliminate coding and algorithmic errors and to identify codes whose assumptions regarding the basic mechanics are inappropriate for the class of problems to be solved. It also showed the importance of using modellers who are knowledgeable in the appropriate field of mechanics and who are experienced with use of the computer code that executes the model.

The program demonstrated the utility of a well-characterized material with little scatter, and showed the necessity of quantifying the precision in tests performed to validate the computer models by making duplicate measurements either in the same test or by repeating the test. It also showed that the precision tests need to produce a variety of data so that more aspects of the models can be validated. This is important because although some quantities may be of secondary importance, accurate predictions of these responses show that the model accurately predicts the primary response for the right reason. This is essential for confidence that the models can make accurate predictions for problem specifications that are different from those included in model development and validation.

Additionally, the program demonstrated the need for sophisticated constitutive models that accurately simulate non-linear material behaviour. More work is needed to develop a consensus on the functional form that best represents various aspects of material behaviour. Finally, it is essential that the experimental results not be known before the model prediction is complete. Because the problems show significant sensitivity to physical and numerical parameters, it is very easy to adjust the prediction of these highly sophisticated computer models to match measurements.

Several shortfalls in the current program have also been uncovered. A major shortfall is that there is no stated accuracy that needs to be demonstrated. This can lead to endless revision of the model without achieving further practical accuracy. The class of problems being solved needs to be well understood and the practical implication of the variability and uncertainty needs to be understood so that required accuracy can be stated.

Another shortfall is that only one material, Salem limestone, was used in the precision tests. This allows for the possibility that the models were tuned to this material behaviour and may in fact have significant prediction error for similar problems in other rock types. Therefore the known credibility of the models is limited to rocks that behave similar to Salem limestone.

Finally, since the models were refined and improved as the program proceeded, the models should have been verified before predicting the jointed-rock precision test because coding or algorithmic errors could have been introduced. This would have been very difficult because the models in each computer code were so different that differences in predictions could not be readily attributed to coding or algorithmic errors. Ideally, model development and validation should be carried out sequentially. Practical considerations, however, often dictate that the development and validation be conducted concurrently, as in the current example. Nonetheless, the model validation process will be more coherent if there is some concurrence that a specific modelling approach is the most appropriate and has been incorporated in several computer codes.

This discussion shows that it is essential that computer models be validated over a wide range of conditions because we rely on the predictions of these models for design or performance assessment of many structures and systems. This is a large and difficult task with little guidance on how to proceed. Other branches of mechanics are aware of the validation problem and have encountered similar difficulties in achieving the level of confidence desired.<sup>55</sup> Clearly, then, models should be developed with care and applied with caution.

## CONCLUSION

A long-term, comprehensive program involving many participants has been carried out to develop and validate computer models for the deformation of structures in jointed rock. The program included computer algorithm development and implementation, parametric studies, constitutive model development, material-properties testing and well-instrumented precision tests.

The predictive capability of three computer models for structures in jointed rock was demonstrated by comparing predictions with the results of a large jointed-rock precision test article that involved loading a lined cylindrical opening. Based on this limited validation, it appears that computer models can accurately simulate several aspects of the deformation of structures in jointed rock. However, confidence in isolated, individual calculations is low because it was not conclusively demonstrated that the accurate predictions that were obtained were arrived at for the correct reasons. In particular, all three computer models predicted the deformed shape of the aluminium liner with acceptable accuracy, but only one model accurately predicted the deformation and fracturing in the limestone. This suggests that confidence is low for predictions of the deformation of unreinforced tunnels.

The program revealed several important generic elements of model development and validation that should be included in any effort to produce computer models that can make reliable predictions for cases involving complex nonlinear mechanical behavior. These elements include:

1. a stated level of accuracy to be demonstrated by the models,
2. a verification effort to find and fix coding and algorithmic errors, which should be repeated after any new coding to incorporate model improvements,
3. modelers who are knowledgeable both in the mechanics being modelled and in operation of the computer code used to implement the model,
4. accurate constitutive models for the materials that include the dependence on rate of deformation, damage and all three stress invariants,
5. precision tests that are performed on well-characterized materials and that produce measurements of a variety of quantities whose precision and accuracy are known, and some of which can be used to determine the boundary conditions, and
6. pre-test predictions by the models to show the *predictive* capability of the models, which is what is desired.

## REFERENCES

1. A. J. Hendron and A. K. Ayer, 'Stresses and strains around a circular tunnel in an elastic-plastic material with dilatancy', DACA 45-59-C-0100, Omaha District Corps of Engineers, Omaha, NE, 1972.
2. C. H. Dowding, T. Belytschko and H. J. Yen, 'A coupled finite element-rigid block method for transient analysis of rock caverns', *Int. J. Numer. Anal. Meth. Geomech.*, **7**, 117-127 (1983).
3. P. A. Cundall and R. D. Hart, 'Development of generalized 2-D and 3-D distinct element program for modeling jointed rock'. *Misc. Paper SL-85-1*, Itasca Consulting Group, US Army Corps of Engineers, 1985.
4. R. Goodman and G.-H. Shi, *Block Theory and its Application to Rock Engineering*, Prentice-Hall, Englewood Cliffs, NJ, 1985.
5. E. Johansson and L. J. Lorig, 'Use of numerical models in design and excavation monitoring of multiple parallel caverns', *Int. Symp. on Unique Underground Structures*, Vol. 1, CSM Press, Golden, CO, 1990, pp. 11-1 to 11-19.
6. H. Duddeck, 'Application of numerical analyses for tunneling', *Int. J. Numer. Anal. Meth. Geomech.*, **15**, 223-239 (1991).
7. D. K. Vaughn and J. Isenberg, 'Stability of openings in jointed rock', *Int. J. Numer. Anal. Meth. Geomech.*, **15**, 433-442 (1991).
8. L. Lorig and C. Fairhurst, 'Three-dimensional discontinuum modeling for underground excavations', in S.-T. Chen et al. (eds), *1992 Rock Engineering Symp. in Taiwan, Tainan*, 1992, pp. 349-358.

9. L. E. Schwer and H. E. Lindberg, 'A finite element slideline approach for calculating tunnel response in jointed rock', *Int. J. Numer. Anal. Meth. Geomech.*, **16**, 529–540 (1992).
10. B. Dasgupta and L. J. Lorig, 'Numerical modelling of underground power houses in India' *Eighth ISRM Int. Congress on Rock Mechanics*, Tokyo, 1995, pp. 65–74.
11. W. Müller 'Numerical modelling of the interaction of rock support with faulted layered rock in coal strata under high convergence', *Proc. 2nd Int. Conf. on the Mechanics of Jointed and Faulted Rock*, Vienna, 1995, pp. 557–561.
12. G. E. Wickham, H. R. Tiedemann and E. H. Skinner, 'Support determination based on geologic predictions', *Proc. Rapid Excav. Tunneling Conf. AIME*, New York, 1972, pp. 43–64.
13. Z. T. Bienawski, 'Engineering classification of jointed rock masses', *Trans. S. Afr. Inst. Civ. Eng.*, **15**, 335–344 (1973).
14. N. R. Barton, R. Lien and J. Lunde, 'Engineering classification of rock masses for the design of tunnel support', *Rock Mech.*, **6**, 189–236 (1974).
15. L. Müller, 'Misconceptions on the New Austrian tunneling method', *Tunnels Tunneling*, **10**, 29–32 (1978).
16. A. M. Starfield and P. A. Cundall, 'Towards a methodology for rock mechanics modelling', *Int. J. Rock Mech. Min. Sci. Geomech. Abstr.* **25**(3), 99–106 (1988).
17. J. K. Gran, P. E. Senseny, M. A. Groethe, D. E. Chitty and J. Trulio, 'Dynamic response of an opening in jointed rock', *Int. J. Rock Mech. Min. Sci. Geomech. Abstr.*, **35**(8), 1021–1035 (1998).
18. P. E. Senseny, M. A. Groethe, S. E. Blouin, D. E. Chitty, J. Trulio, J. K. Gran and G. R. Greenfield 'Dynamic loading test of an opening in a sub-scale jointed rock mass', *Proc. 2nd Int. Conf. on the Mechanics of Jointed and Faulted Rock*, Vienna, 1995, pp. 477–482.
19. O. R. Walton, 'Explicit particle Dynamics Model for Granular Materials', in R. Dungar, G. N. Pande, and J. A. Studer (eds.), *Numerical Methods in Geomechanics A. A. Balkema*, Brookfield, VT, 1982, pp. 1261–1268.
20. Itasca Consulting Group, Inc., UDEC Version 1·8 Users' Manual, Minneapolis, MN, 1992.
21. Y. M. Ito, R. H. England and R. B. Nelson, 'Computational method for soil-structure interaction', *Comput. Struct.*, **13**, 157–162 (1981).
22. D. K. Vaughn and E. Richardson, 'FLEX Users' Manual', *Weidlinger Associates Report*, Version 1-H.2 1991.
23. L. M. Taylor and D. P. Flanagan, 'PRONTO2D: a two-dimensional transient solid dynamics program', SAND86-0594, Sandia National Laboratories, Albuquerque, NM, 1987.
24. P. E. Senseny and D. A. Simons, 'Comparison of calculational approaches for structural deformation in jointed rock', *Int. J. Numer. Anal. Meth. Geomech.*, **18**, 327–344 (1994).
25. D. A. Simons, 'Numerical and analytical solutions to benchmark problems related to tunnel mechanics', *DNA-TR-92-176*, RDA, 1993.
26. T. A. Pućik, T. F. Curry, S. T. Dziuban and P. E. Senseny, 'The use of experimental design in large-scale finite element simulations', *Proc., 1994 Summer Computer Simulation Conf.*, Society for Computer Simulation, San Diego, CA, 1994, pp. 916–920.
27. I. S. Sandler and D. Rubin, 'An algorithm and a modular subroutine for the cap model', *Int. J. Numer. Anal. Meth. Geomech.*, **3**, 173–186 (1979).
28. A. F. Fossum, P. E. Senseny, T. W. Pfeifle and K. D. Mellegard, 'Experimental determination of probability distributions for parameters of a Salem limestone cap plasticity model', *Mech. Mater.*, **21**, 119–137 (1995).
29. D. E. Chitty, S. E. Blouin, X. Sun and K. J. Kim, 'Laboratory investigation and analysis of the strength and deformation of joints and fluid flow in Salem limestone', *DNA-TR-93-63*, Applied Research Associates, 1994.
30. J. K. Gran, M. A. Groethe, D. Chitty and J. G. Trulio, 'MIGHTY NORTH 1 Precision Test', *DSWA-TR-96-63*, SRI International 1997.
31. J. W. Simons, L. Seaman, P. R. Gefken, and AL. Florence, 'Tunnel tests in limestone', *DNA-TR-92-164*, SRI International, 1992.
32. P. E. Senseny, H. E. Lindberg, and T. C. Kennedy, 'A machine for static and dynamic triaxial testing', *Exp. Mech.*, **19**(2), 63–68 (1979).
33. R. W. Klopp, J. W. Simons, A. L. Florence and J. K. Gran, 'Laboratory tests in support of the underground technology program (UTP)', *DNA-TR-94-183-Rev.*, SRI International, 1994.
34. R. W. Klopp, A. L. Florence, J. W. Simons and J. K. Gran, 'Spherical wave interaction with cylindrical holes in large limestone specimens', *J. Phy. IV, Colloque C8, supplément au Journal de Physique III*, **4**, C8-735-C8-740 (1994).
35. R. G. Whirley, 'DYNA3D: a nonlinear, explicit three-dimensional finite element code for solid mechanics users manual', *Technical Report UCRL-MA-107254*, Lawrence Livermore National Laboratory 1991.
36. D. Pelessone, 'A modified formulation of the cap model', *Technical Report GA-C19579*, General Atomics, 1989.
37. L. E. Schwer and Y. D. Murray, 'A three-invariant smooth cap model with mixed hardening', *Int. J. Numer. Anal. Meth. Geomech.*, **18**, 657–688 (1994).
38. M. B. Rubin, 'Simple, convenient isotropic failure surface', *J. Engng. Mech.*, **117**, 348 (1991).
39. K. J. Willam and E. P. Warnke, 'Constitutive model for the triaxial behavior of concrete', *Proc. Int. Association of Bridge and Structural Engineers*, Vol. **19**, Seminar on Concrete Structure Subjected to Triaxial Stresses, Paper III-1, Bergamo, Italy, 1975.
40. W. F. Chen and D. J. Han, *Plasticity for Structural Engineers*, Springer, New York, 1988.

41. J. C. Mould and H. S. Levine, 'A rate-dependent three-invariant softening model for concrete', in G. Voyiadjis *et al.* (eds.), *Studies in Applied Mechanics, Mechanics of Materials and Structures*, Elsevier, Amsterdam, 1994.
42. ABAQUS Theoretical Manual, Version 5.4, Hibbitt, Karlsson & Sorenson, 1994.
43. S. J. Green and R. D. Perkins, 'Uniaxial compression tests at varying strain rates on three geological materials', in R. E. Gray (ed.), *Basic and Applied Rock Mechanics*, 1972.
44. G. Duvaut and J. L. Lions, *Inequalities in Mechanics and Physics*, Springer, New York, 1972.
45. Y. M. Ito and Y. Muki, 'Damage model for explosive interactions', *Proc. 8th Int. Symp. on Interaction of Effects of Munitions with Structures*, McLean, VA, 1997.
46. J. C. Simo, J.-W. Ju, K. S. Pister and R. L. Taylor, 'An assessment of the cap model consistent return algorithms and rate-dependent extensions', *J. Engng Mech.* **114**, (1988).
47. H. D. Zimmerman, Y. M. Ito, J. A. Carney and J. E. Windham, 'Enhanced constitutive models on calculated ground shock', *Proc. 6th Int. Symp. on Interaction of Non-Nuclear Munitions with Structures*, Panama City Beach, FL, 1993.
48. J.-W. Ju, 'On energy-based coupled elastoplastic damage theories: constitutive modeling and computational aspects', *Int. J. Solids Struct.* **25**(7), (1989).
49. Y. M. Ito, Muki and R. B. Nelson, 'Dynamic modeling: solids with discontinuities', *Proc. Numerical Methods in Structural Mechanics at 1st Joint Applied Mechanics and Materials Summer Conf.* University of California, Los Angeles, CA, 1995.
50. J. Weerheijm, J. C. A. M. van Doormaal and L. J. Sluys, 'Fracture energy of concrete under dynamic tensile loading', *Proc. 6th Int. Symp. on Interaction of Non-Nuclear Munitions with Structures*, Panama City Beach, FL, 1993.
51. Y. M. Ito, R. H. England and R. B. Nelson, 'Computational method for soil-structure interaction problems', *Comput. Struct.* **13**(1-3) (1981).
52. D. Tennant, H. S. Levine and J. C. Mould Jr., 'Prediction of static and dynamic response of reinforced concrete slabs using a rate-dependent three-invariant softening model for concrete', *Proc. 8th Int. Symp. on Interaction of the Effects of Munitions with Structures*, McLean, VA, 1997, p. 147.
53. H. S. Levine, C. J. Ludwig, D. K. Vaughan and J. Isenberg, 'Comparison of two different approaches for interface modeling in large in large scale soil structure interaction problems', in A. K. Noor and H.S. Levine (eds), *Large Scale Interaction Problems*, AMD Vol. 94, 1988, pp. 1-22.
54. P. A. Vermeer and R. de Borst, 'Non-associated plasticity for soils, concrete and rock', *Heron*, **29**(3), 3-64 (1984).
55. C. J. Freitas, 'Perspective: selected benchmarks from commercial CFD codes', *ASME J. Fluids Engng.*, **117**, 208-218 (1995).